Fracture Behavior and Deformation Mechanism of Polypropylene/Ethylene–Octene Copolymer/Magnesium Hydroxide Ternary Phase Composites

Jun Yin, Yong Zhang, Yinxi Zhang

School of Chemistry and Chemical Technology, Shanghai Jiao Tong University, Shanghai 200240, People's Republic of China

Received 17 August 2004
DOI 10.1002/app.22111
Published online in Wiley InterScience (www.interscience.wiley.com).

ABSTRACT: The fracture behavior and deformation mechanism of polypropylene (PP)/ethylene–octene copolymer (POE)/magnesium hydroxide [$Mg(OH)_2$] ternary composites were investigated. The fracture behavior of the PP/POE/$Mg(OH)_2$ ternary composites was strongly influenced by the POE content. In the case of brittle fracture, the debonding of filler particles dominated the deformation process. Strong shear yielding of the matrix ligaments between microvoids took place after the brittle–ductile transition. The existence of POE could improve the deformability of the PP matrix and change the debonding manner of the filler particles. The fracture behavior of the PP/POE composites was investigated by the single-edge notch tensile test at 1 mm/s (a low test speed). The introduction of POE led to a decrease in the crack initiation energy and an increase in the crack propagation energy. The improvement in the fracture energy with increasing POE content was dominated by the increase in the crack propagation energy. A morphology analysis of the PP/POE composites demonstrated that a mixture of separation and encapsulation microstructures existed in the matrix. © 2005 Wiley Periodicals, Inc. J Appl Polym Sci 98: 957–967, 2005

Key words: poly(propylene) (PP); composites; fracture; deformation mechanism

INTRODUCTION

Inorganic fillers can provide polymers with modified physical properties and specific functions, such as flame retardancy. Magnesium hydroxide [$Mg(OH)_2$] has been proved to be an effective flame retardant for the flame resistance of polypropylene (PP). However, an excessive loading level of $Mg(OH)_2$ is essential for desired flame retardancy, but it leads to a dramatic deterioration in the mechanical properties of PP, especially in toughness. On the other hand, the improvement in the impact strength by the introduction of elastomers is accompanied by a simultaneous decrease in the modulus, which can be compensated by the addition of a filler or reinforcement.[1] Therefore, PP/elastomer/rigid filler ternary composites with potentially outstanding mechanical properties have attracted increasing interest because of their applicative importance.

The properties and microstructures of PP/elastomer/inorganic filler ternary composites are dominated by the mutual miscibility and adhesion of the components.[2] Three types of microstructures are assumed in PP ternary composites: (1) a separated microstructure in which the elastomer and filler particles are dispersed separately in the polymer matrix, (2) a core–shell microstructure in which the elastomer encapsulates the filler particles and leads to a soft interlayer between the matrix and filler, and (3) a mixture of separated and core–shell microstructures.[3] Many investigations have suggested that the final structure is determined by the adhesion between the phases and the stability of the encapsulated units against shear forces in the melt during the mixing process.[4,5]

The PP–filler or elastomer–filler interfacial adhesion is another important factor controlling the microstructures of PP ternary composites. The increase in adhesion between PP and the filler will lead to a separated dispersion microstructure of the filler and elastomer particles in the matrix, whereas an encapsulation microstructure will be preferred when adhesion between the elastomer and filler increases.[6,7] Functionalized polymers are usually introduced into PP ternary composites to adjust the interfacial adhesion between the components. The difference in the microstructures results in different mechanical properties; however, the effects of the microstructure on the composite properties are rather controversial. It is believed that the composites with an encapsulation structure have higher impact strength and lower modulus than those with a separation structure because of the increased

Correspondence to: J. Yin (cupidyin@sjtu.edu.cn).

© 2005 Wiley Periodicals, Inc.

elastomer apparent content extended by filler particles.[8] However, Jancar and Dibenedetto[9] studied PP/ethylene–propylene–diene terpolymer (EPDM)/filler ternary composites containing 30 vol % fillers [$CaCO_3$ and $Mg(OH)_2$]. The results indicated that both the modulus and impact strength of the PP composites with a separation structure were higher than those of the composites with an encapsulation structure. Wang et al.[10] studied the mechanical properties of PP/elastomer/$Mg(OH)_2$ ternary composites. Functionalized ethylene–propylene rubber (EPR) reacted with the surface of uncoated $Mg(OH)_2$, and this led to extensive rubber encapsulation and an improvement in the toughness with respect to unmodified EPR. However, through the blending of functionalized EPR with a filler surface-treated with magnesium stearate, encapsulation was inhibited, and the rubber was preferentially dispersed in the PP matrix. This formulation resulted in both improved filler–matrix interaction and enhanced matrix toughening, leading to a further increase in the impact strength. Dubnikova et al.[11] studied the correlation between the morphology and the impact toughness for PP/EPR/glass bead ternary phase composites. The stress of start of local failure microprocesses at the inclusion–matrix boundary was found to play the dominating role in energy-dissipating mechanisms. The optimal stiffness–toughness balance could be obtained via the coating of the rigid particles with an elastomer shell.

In this study, the fracture behavior and deformation mechanism of PP/ethylene–octene copolymer (POE)/$Mg(OH)_2$ ternary composites were investigated. The deformation mechanism and dispersion microstructure of the PP/POE composites were analyzed with scanning electron microscopy (SEM). The fracture behavior of the ternary composites was studied with the single-edge notch tensile (SENT) test. In addition, a toughening mechanism for the PP/POE/$Mg(OH)_2$ ternary composites was proposed.

EXPERIMENTAL

Materials

PP (PP 1304E1) was a homopolymer supplied by ExxonMobil Chemical (Houston, TX). Its density and melt flow index (2.16 kg at 230°C) were 0.9 g/cm^3 and 11 g/10 min, respectively. $Mg(OH)_2$ (Magnifin H5, Bergheim, Germany) was a high-purity, platelike powder without surface modification supplied by Martinswerk GmbH Co. (Bergheim, Germany). The average particle size and Brunauer–Emmett–Teller specific surface area were 1.25–1.45 μm and 4.0–6.0 m^2/g, respectively. The elastomer was POE (EG8180) supplied by Du Pont–Dow Elastomer Co. (Midland, MI). Its octane content and nominal Mooney viscosity [ML(1 + 4)] at 121°C were 42 wt % and 35, respectively. Stearic acid (SA) was used as the surface modifier.

Blending and specimen preparation

The $Mg(OH)_2$ filler was pretreated with 1 wt % SA before compounding. The PP/POE/$Mg(OH)_2$ ternary composites with various POE and filler contents were prepared with a Berstoff ZE25A corotating twin-screw extruder (length/diameter = 41, diameter = 25 mm; Berstoff, Hannover, Germany) with a temperature profile of 180/190/200/200/200/200/190/200°C and a rotating speed of 250 rpm; this gave a melt temperature of about 220°C. The extrudates were pelletized and dried in a vacuum oven at 80°C for 18 h for specimen preparation.

The test specimens for morphology observation and mechanical property testing were injection-molded on an injection-molding machine. The temperatures of the barrel and mold were set at 220 and 40°C, respectively. Before the mechanical property testing, the specimens were dried at 23°C *in vacuo* for 18 h.

Mechanical properties

The tensile properties were determined with an Instron 4465 tensile machine (Instron Corp., Canton, MA) according to ASTM D 638 at a crosshead speed of 50 mm/min and a testing temperature of 20°C. The dimension of the dumbbell bar followed ASTM D 638M-93 type M-II. The gauge length, width, and thickness of the dumbbell tensile bars were 25, 6, and 2 mm, respectively.

The notched Izod impact specimens had a 2-mm-deep, 45° V-shape notch and a notch tip radius of 0.25 mm on rectangular bars ($80 \times 10 \times 4$ mm^3) according to ISO 178. The test was performed with a Ray-Ran impact test (Ray-Ran Test Equipment, Ltd., Nuneaton, United Kingdom) according to ISO 180 with an impact velocity of 3.5 m/s and a pendulum weight of 0.818 kg at a testing temperature of 23°C. The test results were the average data of five samples.

SENT test

The fracture behavior of the PP/POE/$Mg(OH)_2$ composites was studied with a tensile test on the notched impact specimens. The procedures of the SENT test can be found in the literature.[12] The notched Izod specimens ($74 \times 10 \times 4$ mm^3), with a 2-mm-deep, 45° V-shape notch and a notch tip radius of 0.25 mm, were used according to ISO 180/1A. The SENT test was carried out on the notched Izod specimens with a clamp length of 45 mm at a low crosshead speed of 1 mm/s. Each test was carried out five times.

A schematic illustration of a stress–displacement curve measured from the SENT test is given for a

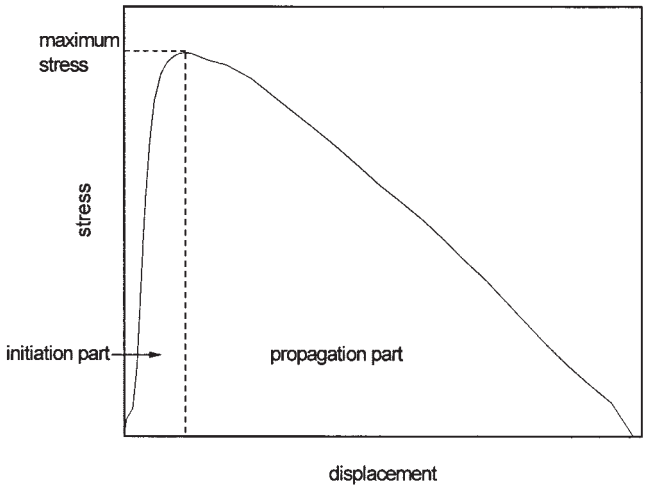

Figure 1 Typical stress–displacement curve of a SENT test for the PP/POE/$Mg(OH)_2$ composites.

tough fractured sample in Figure 1. The maximum stress was recorded, and the fracture energy was calculated by the integration of the force and displacement signals. The fracture energy was divided into an initiation part and a propagation part. The point of maximum stress was chosen as the boundary between crack initiation and crack propagation. In the case of brittle behavior, the stress fell almost immediately from the maximum stress to zero, and this indicated very low crack propagation energy.[13]

Morphology observation

The phase morphology and fracture behavior of the PP/POE/$Mg(OH)_2$ composites were studied by SEM analysis. The samples for phase morphology observation were prepared from notched impact specimens that were immersed in liquid nitrogen and fractured under high-speed impact. To measure the elastomer particle size and its distribution, the samples were etched in boiling *n*-heptane for 1 h to remove POE. After drying at 80°C *in vacuo* for 12 h, the samples were gold-coated and observed with a Hitachi S-2150 scanning electron microscope (Hitachi, Tokyo, Japan) with an accelerating voltage of 15 kV. The particle size was then determined from the micrographs with graphic analysis on a computer.

For the fracture behavior analysis, the samples were prepared by a notched Izod impact test at 23°C. All the surfaces were then gold-coated and observed with a Hitachi S-2150 SEM instrument with an accelerating voltage of 15 kV. The observations were focused on the regions ahead of the notch tip of the impact-fracture specimen.

RESULTS AND DISCUSSION

Influence of POE on the toughness of PP/POE/$Mg(OH)_2$ ternary composites

The toughness of particulate polymer composites depends on the interfacial adhesion between the polymer matrix and filler and the deformability of the polymer matrix under an external force. Because of the restrained deformability of the PP matrix and the weak adhesion between the PP matrix and filler, PP/$Mg(OH)_2$ composites exhibit poor fracture toughness, especially under notched test conditions. POE is used to modify the toughness of the composites, and the dependence of the impact strength of PP/POE/$Mg(OH)_2$ ternary composites on the POE content is shown in Figure 2. As the POE content increases to 30 phr, the impact strength of PP/POE composites increases from 26 to 425 J/m, and this indicates a significant improvement in the toughness. This behavior is similar to the cases of polymers toughened with rubber.[14,15] The differential analysis of the impact strength of the PP/POE composites suggests that a brittle–ductile transition occurs in the PP/POE (80/20 w/w) composites. With further increasing POE content, the PP/POE composites could be fractured in a ductile manner, and the even became unbroken. However, because of the existence of soft POE particles, the tensile yield strength and Young's modulus almost decrease linearly with increasing POE content, as shown in Figures 3 and 4.

Stress whitening was observed on the specimens of all the composites after impact fracture. The influence of the POE content on the stress-whitening zone of the composites is schematically illustrated in Figure 5. In the PP composite, stress whitening only occurs around the notch tip. No stress whitening was observed on

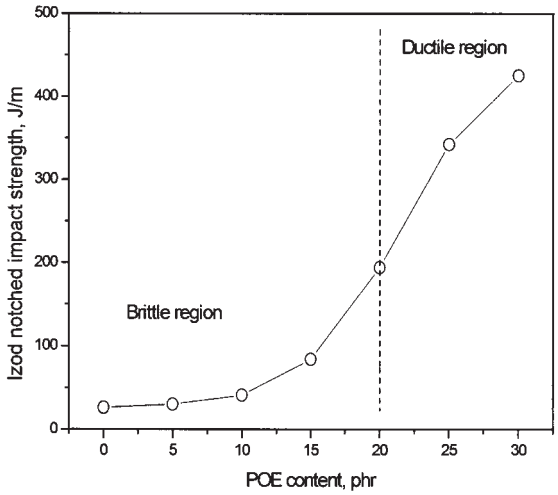

Figure 2 Dependence of the notched Izod impact strength on the POE content in the PP/POE/$Mg(OH)_2$ composites [formulation: PP + POE = 100 phr, $Mg(OH)_2$ = 120 phr].

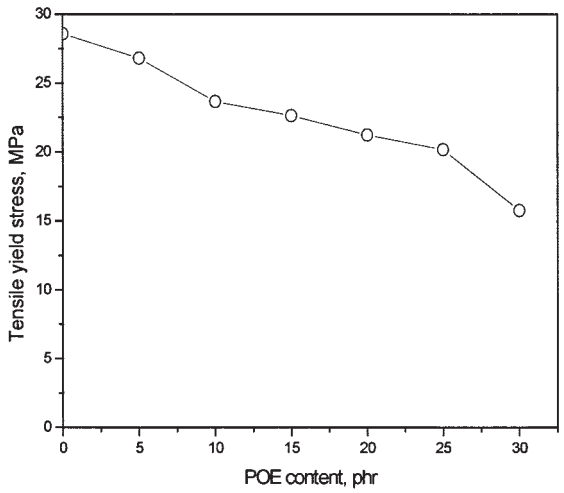

Figure 3 Dependence of the tensile yield stress on the POE content in the PP/POE/$Mg(OH)_2$ composites [formulation: PP + POE = 100 phr, $Mg(OH)_2$ = 120 phr].

the profile of impact specimens, except on the end region. The stress whitening observed on the end region of the specimens might be attributed to the uniaxial tension on the PP matrix during the impact-fracture process. With increasing POE content, the stress-whitening zone extends over the whole fracture surface. Obvious stress whitening was first observed in the PP/POE (85/15 w/w) composite. Because of the tensile stress around the end field, a triangular zone of stress whitening appeared close to the fracture surface. The thickness of the stress-whitening zone increased with increasing POE content. In addition, the shape of the stress-whitening zone changed from triangular to elliptical. The results indicate the improvement of POE in the plastic deformability of the polymer matrix.

The matrix properties also play an important role in the impact behavior of PP/POE composites. A PP/POE (70/30 w/w) blend is used as the matrix, and the influence of the $Mg(OH)_2$ content on the impact strength of the PP/POE composites is shown in Figure 6. The impact strength of the PP/POE composites first increases with increasing $Mg(OH)_2$ content, but at a higher loading of $Mg(OH)_2$, the impact strength decreases. The increase in the impact strength should be related to the debonding behavior of filler particles induced by stress concentration in the matrix during the deformation process. The toughening model of semicrystalline polymers developed by Muratoglu et al.[16] suggests that the roles of rubber particles in toughening the polymer matrix provide the interpenetrating layers of the crystalline matrix around themselves and offer no constraint to the deforming matrix ligaments by cavitation at the start of deformation, which can be replaced by rigid particles providing the same percolation conditions for plastic deformation of semicrystalline polymers. Thus, the formation of microvoids caused by the debonding of filler particles improves the plastic deformation of the matrix ligaments toughened with POE, and this results in an increase in the impact strength of the PP/POE composites. The interfacial adhesion between $Mg(OH)_2$ and the PP or POE matrix should play an important role in the toughness of the PP/POE composites. That is why a high $Mg(OH)_2$ content led to a considerable reduction in the impact strength of the composites.

Deformation mechanism of PP/POE/$Mg(OH)_2$ ternary composites

The toughening of semicrystalline polymers with rubber particles has been successfully explained by the percolation theory.[14,15] However, for polymer/elastomer/filler ternary composites, the micromechanical deformation and toughening mechanism are more complicated because of the coexistence of rubber and rigid particles. Investigations of the deformation mechanism were performed with SEM analysis of the impact-fracture surfaces of PP/POE/$Mg(OH)_2$ composites with various POE contents, as shown in Figure 7. In the PP composites [Fig. 7(a)], a large number of microvoids formed during the fracture process caused by the debonding of filler particles from the matrix, and no considerable plastic deformation of the ligaments between the microvoids was observed; this resulted in poor impact strength. The addition of a small amount of POE changed the deformation process of the PP/POE composites dramatically. As shown in Figure 7(b,c), fibril-like structures formed, surrounding the filler particles debonding from the matrix in the composites containing 10 and 15 phr POE. Moreover, the matrix ligaments exhibited considerable

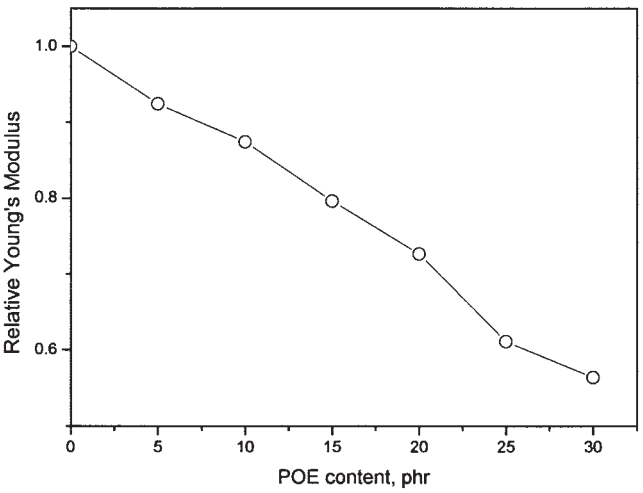

Figure 4 Dependence of the relative Young's modulus on the POE content in the PP/POE/$Mg(OH)_2$ composites [formulation: PP + POE = 100 phr, $Mg(OH)_2$ = 120 phr].

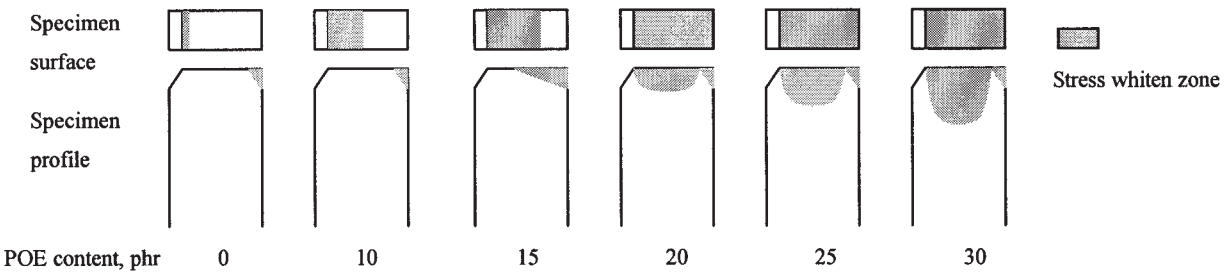

Figure 5 Schematic illustration of the influence of the POE content on the development of the stress-whitening zone after impact fracture.

plastic deformability during the fracture process. With further increasing POE content [Fig. 7(d–f)], extensive shear flows of the polymer matrix were observed, indicating a transition from a brittle fracture manner to a ductile fracture manner for the PP/POE composites. Significant plastic deformation due to the shear deformation of the polymer matrix led to an increase in the impact energy consumed during the deformation process and, consequently, a significant increase in the impact strength of the PP/POE composites. The debonding degree of $Mg(OH)_2$ particles dramatically decreased in the PP/POE composites with high POE contents. As shown in Figure 7(f), many filler particles immersed in the matrix instead of debonding from the matrix during the deformation process. The restraint in debonding was due to the existence of POE and could weaken the influence of the filler particles on the deformation process of the PP/POE composites.

The influence of POE on the deformation mechanism of PP/POE composites must be considered from two aspects, that is, the filler particle debonding behavior and the deformability of the matrix. Because the influence of POE on the deformability is similar to that of a rubber-toughened polymer, the discussion is focused on the influence of POE on $Mg(OH)_2$ particle debonding. A schematic representation of $Mg(OH)_2$ particle debonding behavior is given in Figure 8. For the PP composites, the interfacial adhesion between the filler and polymer matrix is poor. Because of the undeformability of the rigid filler particles, the maximum stress concentrates in the polar regions of the particles, where the particle debonding is initiated and followed by the formation of microvoids. The debonding of the filler particles from the polymer matrix releases the strain restricted in ligaments surrounding the particles and leads to a transition of the stress state from triaxial tension to biaxial or uniaxial stress, which stretches the microvoids.[17] However, because of the restrained deformability of PP, the sizes of the microvoids are slightly different from those of the filler particles [Fig. 7(a)]. For the PP/POE composites with low POE contents, the debonding process of filler particles was accompanied with fibrillation at the interface between the filler and polymer matrix. The existence of fibrils that formed at the interface suggests an improvement in the deformability of the polymer matrix and the interfacial adhesion between the filler and polymer matrix. The fibrillation structure was also observed in PP/EPDM blends by Kim and Micher.[17] They demonstrated that fibrillation at the interface between the modifier particles and matrix can occur in blends with a certain phase adhesion, which is simultaneously accompanied by a debonding process. To evaluate the improvement of POE in the interfacial adhesion of PP/POE composites, a semiempirical correlation developed by Pukanszky and coworkers[18,19] and based on the composition dependence of the tensile yield stress in heterogeneous polymer systems is introduced:

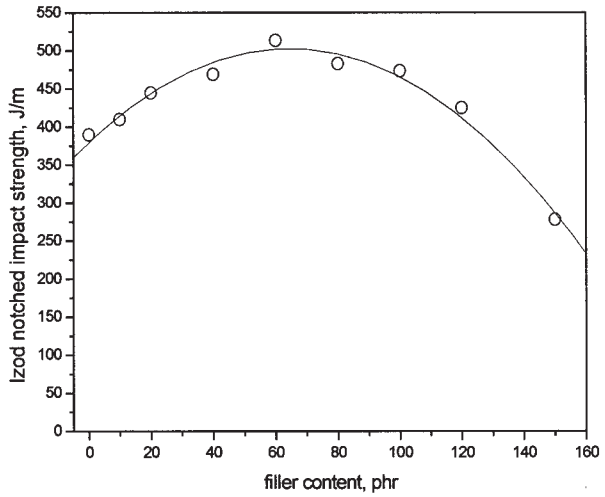

Figure 6 Dependence of the notched Izod impact strength on the $Mg(OH)_2$ content in the PP/POE/$Mg(OH)_2$ composites (formulation: PP/POE = 70/30 w/w).

$$\sigma_c = \sigma_m \frac{1 - \varphi_f}{1 + 2.5\varphi_f} \exp(B_y \varphi_f) \quad (1)$$

where σ_c and σ_m are the yield stresses of the composite and polymer matrix, respectively; Φ_f is the volume content of the filler; and B is an empirical parameter

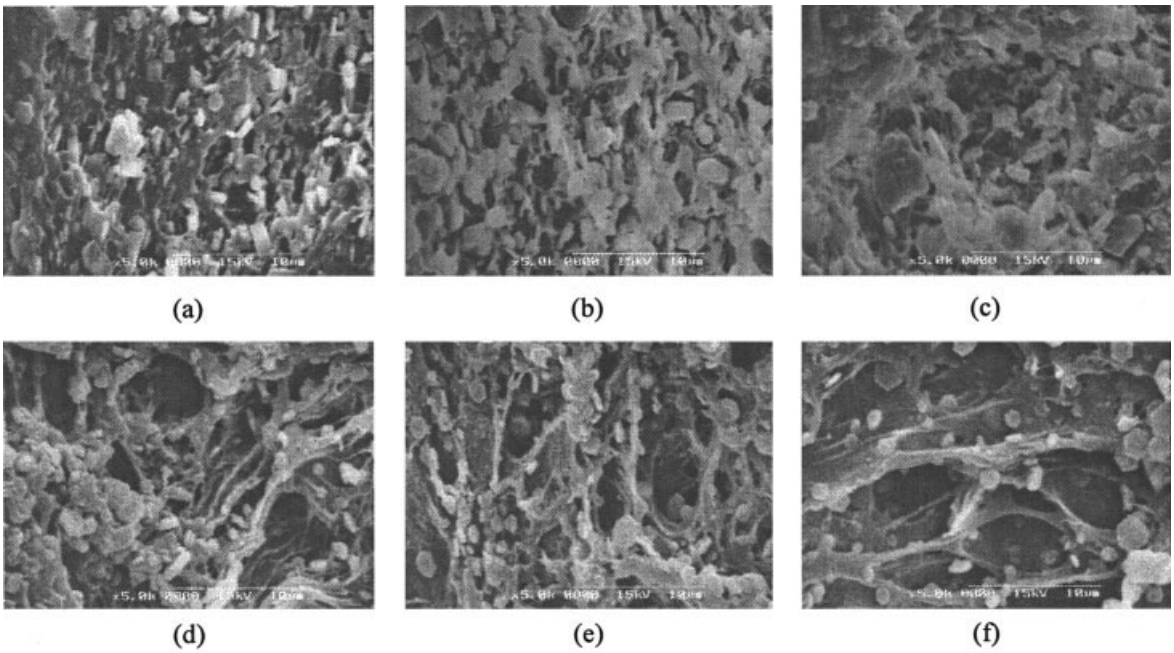

Figure 7 SEM micrographs of the impact-fracture surface on the zone ahead of the notched crack tip of PP/POE/$Mg(OH)_2$ composites with various POE contents at a 5000× magnification: (a) PP/$Mg(OH)_2$ = 100/120, (b) PP/POE/$Mg(OH)_2$ = 90/10/120, (c) PP/POE/$Mg(OH)_2$ = 85/15/120, (d) PP/POE/$Mg(OH)_2$ = 80/20/120, (e) PP/POE/$Mg(OH)_2$ = 75/25/120, and (f) PP/POE/$Mg(OH)_2$ = 70/30/120. The notched crack tip is on the left edge of the micrograph.

related to stress transfer and proportional to interfacial adhesion. A linear plot of $\ln[\sigma_{rel} = \sigma_c(1 + 2.5\Phi_f)/\sigma_m(1 - \Phi_f)]$ (where σ_{rel} is the relative tensile stress) against the filler volume content is presented in Figure 9, and parameter B has been calculated as the slope of a linear curve. For comparison, the PP composites and the PP/POE (70/30 w/w) composites were used. The results demonstrate the improvement of POE in the interfacial adhesion between the filler and polymer matrix. The enhancement of interfacial adhesion by POE promotes the formation of fibrils surrounding filler particles, leading to a considerable increase in the impact strength of the PP/POE composites. The disappearance of particle debonding behavior in the PP/POE composites with higher POE contents might be attributed to the result of excessive improvement in the interfacial adhesion between the filler and matrix. The filler particle debonding is dominated by debonding stress, which depends on the interfacial adhesion between the filler and matrix.[20] The improvement in

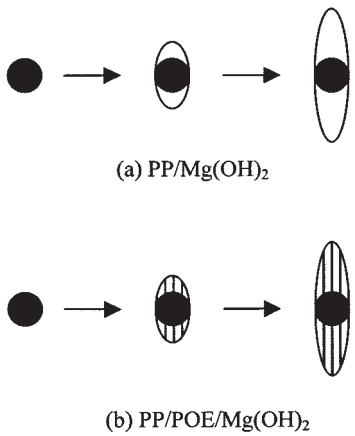

Figure 8 Schematic illustration of filler particle debonding behavior in (a) PP/$Mg(OH)_2$ composites and (b) PP/POE/$Mg(OH)_2$ composites.

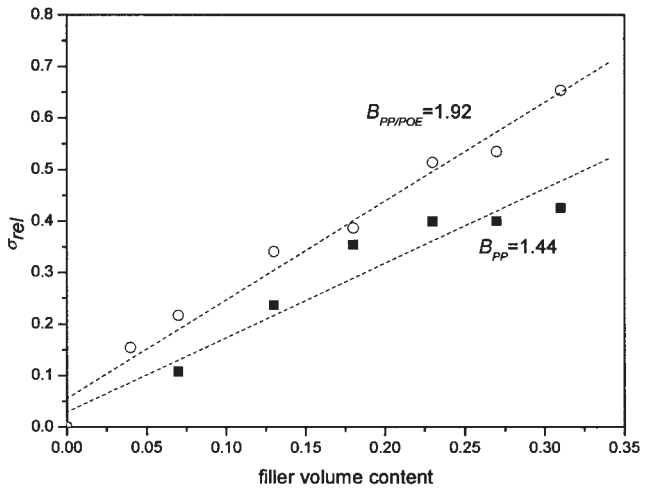

Figure 9 Dependence of σ_{rel} of PP/POE/$Mg(OH)_2$ composites on the filler volume content: (■) PP/POE = 100/0 and $Mg(OH)_2$ = 120 phr and (○) PP/POE = 70/30 and $Mg(OH)_2$ = 120 phr.

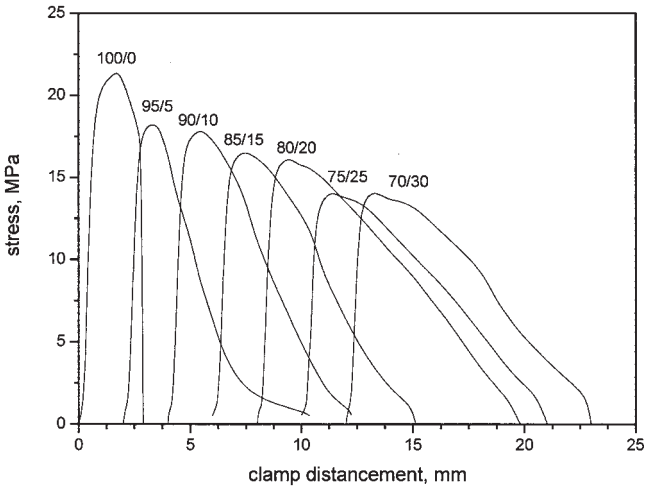

Figure 10 Stress–displacement curves of SENT estimation (1 mm/s) for PP/POE/$Mg(OH)_2$ composites with various POE contents [formulation: PP + POE = 100 phr, $Mg(OH)_2$ = 120 phr].

the interfacial adhesion by POE leads to an increase in the debonding stress, which restricts the filler particle debonding process. On the other hand, the incorporation of POE resulted in a dramatic decrease in the tensile yield stress (Fig. 3). Once the debonding stress is higher than the tensile yield stress, the yielding of the matrix first takes place, rather than the debonding of filler particles. Thus, the debonding process is hindered.

SENT test

To study the influence of POE on the crack initiation and propagation of the PP/POE composites, a SENT test at a low test rate (1 mm/s) was carried out. The stress–displacement curves of the PP/POE composites are shown in Figure 10. The PP composites are fractured in brittle behavior immediately after yielding with a very low crack propagation energy, whereas the stress–displacement curves of the PP/POE composites show typical ductile behavior. With increasing POE content, the displacement increases significantly, and this is accompanied by a considerable reduction in the maximum stress.

The energy and stress analysis results of the PP/POE composites are shown in Figure 11. The incorporation of POE into the composites led to an increase in the fracture energy and a decrease in the maximum stress [Fig. 11(a,b)]. The decrease in the maximum stress can be attributed to the cavitation of POE at relatively low stress with consequent plastic deformation at an early stage of the deformation process.[21] The increase in the fracture energy must be considered from the influence of POE on both the crack initiation energy and crack propagation energy, as shown in Figure 11(c,d). The addition of POE decreased the crack initiation energy of the PP/POE composites, and this may be attributed to the cavitation of POE at an early stage of the deformation process, as mentioned before. On the other hand, the crack propagation energy significantly increased with increasing POE content [Fig. 11(d)]. This can be attributed to high energy dissipation during the crack propagation process due to the shear flow of the matrix and fibrillation surrounding the filler particles (Fig. 7). The energy analysis results indicate that the improvement of the toughness of the PP/POE composites by POE was mainly dominated by its improvement in the crack propagation resistance, rather than the crack initiation resistance.

The sensitivities of all parameters to the POE content decrease with increasing POE content. For the PP/POE composites with a high POE content, all the parameters tend to reach a plateau. This is quite different from the result of the notched impact test (Fig. 2), which shows the brittle–ductile transition in the PP/POE (80/20 w/w) composites. The contradiction might be attributed to the difference in the deformation rates. For the low and intermediate deformation rates, a low rubber content is already sufficient for toughening the polymer, and a high rubber content actually appears not to give optimal fracture energy.[13]

To study the influence of the filler on the toughening of the PP/POE composites, the dependence of the energy and stress analysis results of the PP/POE (70/30) composites on the filler content was also investigated, as shown in Figure 12. With increasing filler content, the maximum stress and crack initiation energy of the PP composites linearly decreased. Besides the weak adhesion between the filler and matrix, the dramatic deterioration in the crack initiation energy can also be attributed to the negative effect of filler debonding on the crack initiation resistance, which obviously depends on the filler content. However, the dependence of the fracture energy and crack propagation of the PP composites on the filler content shows different manners. For the high stereoregularity of the PP matrix, the fracture occurs immediately after the yielding of the matrix, and the crack propagation energy is almost zero. The debonding of the filler particles can improve the deformability of the matrix. In addition, the existence of filler particles can alter the crystalline behavior of PP as an effect of nucleation and improve the deformability of the matrix. Thus, the crack propagation energy increases with increasing filler content, as shown in Figure 12(d). The maximum crack propagation energy appearing in the curve suggests competition between the improvement in the matrix deformability and the poor interfacial adhesion between $Mg(OH)_2$ and the polymer matrix, which leads to a complicated behavior in the dependence of the fracture energy on the filler content [Fig. 12(a)].

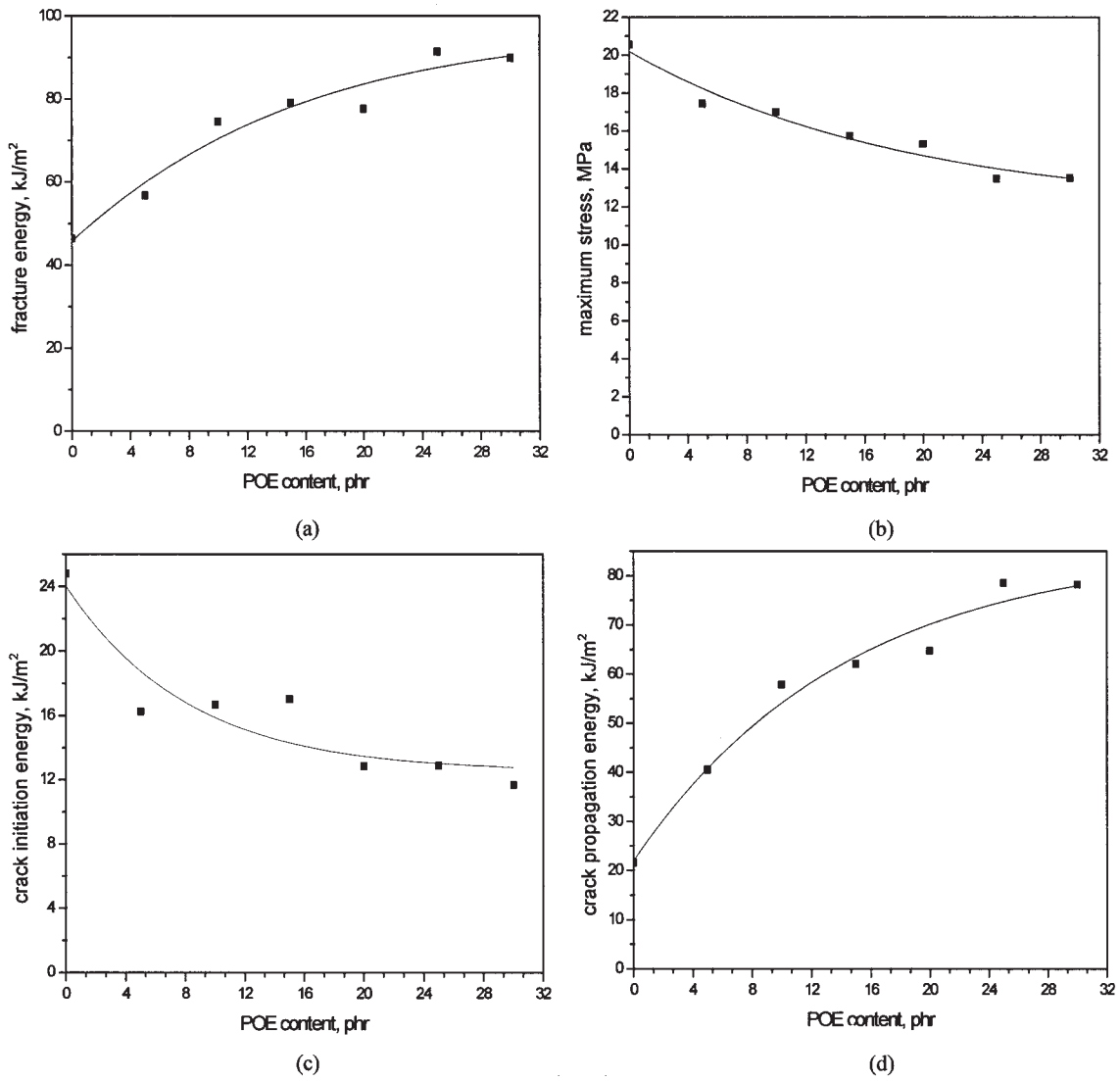

Figure 11 Energy and stress analysis based on the SENT test (1 mm/s) of PP/POE/$Mg(OH)_2$ composites with various POE contents: (a) the total fracture energy versus the POE content, (b) the maximum stress versus the POE content, (c) the crack initiation energy versus the POE content, and (d) the crack propagation energy versus the POE content [formulation: PP + POE = 100 phr, $Mg(OH)_2$ = 120 phr].

The influence of the filler content on the maximum stress and crack initiation energy of PP/POE composites is similar to that of the PP composites. With increasing filler content, the maximum stress and crack initiation energy decreased, independently of the properties of the polymer matrix. However, the dependence of the crack propagation energy of the PP/POE composites on the filler content is quite different. The crack propagation energy first increased with increasing filler content, and this was followed by a decrease at a high filler content. This is in agreement with the results of the notched impact test (Fig. 6). Because of the dramatic deterioration in the crack initiation energy of the PP/POE composites, the fracture energy continually decreased with increasing filler content.

Morphology analysis

To study the microstructure of the PP/POE/$Mg(OH)_2$ composites, POE was selectively extracted with boiling *n*-heptane. The morphology of the PP/POE composites with various POE contents is shown in Figure 13. The number-average (D_n) and weight-average (D_w) particle sizes were calculated, and the results are shown in Table I. Those average particle sizes are defined as follows:

$$D_n = \frac{\sum n_i d_i}{\sum n_i} \quad D_w = \frac{\sum n_i d_i^2}{\sum n_i d_i}, \tag{2}$$

where n_i and d_i were the number and diameter of POE particle, respectively.

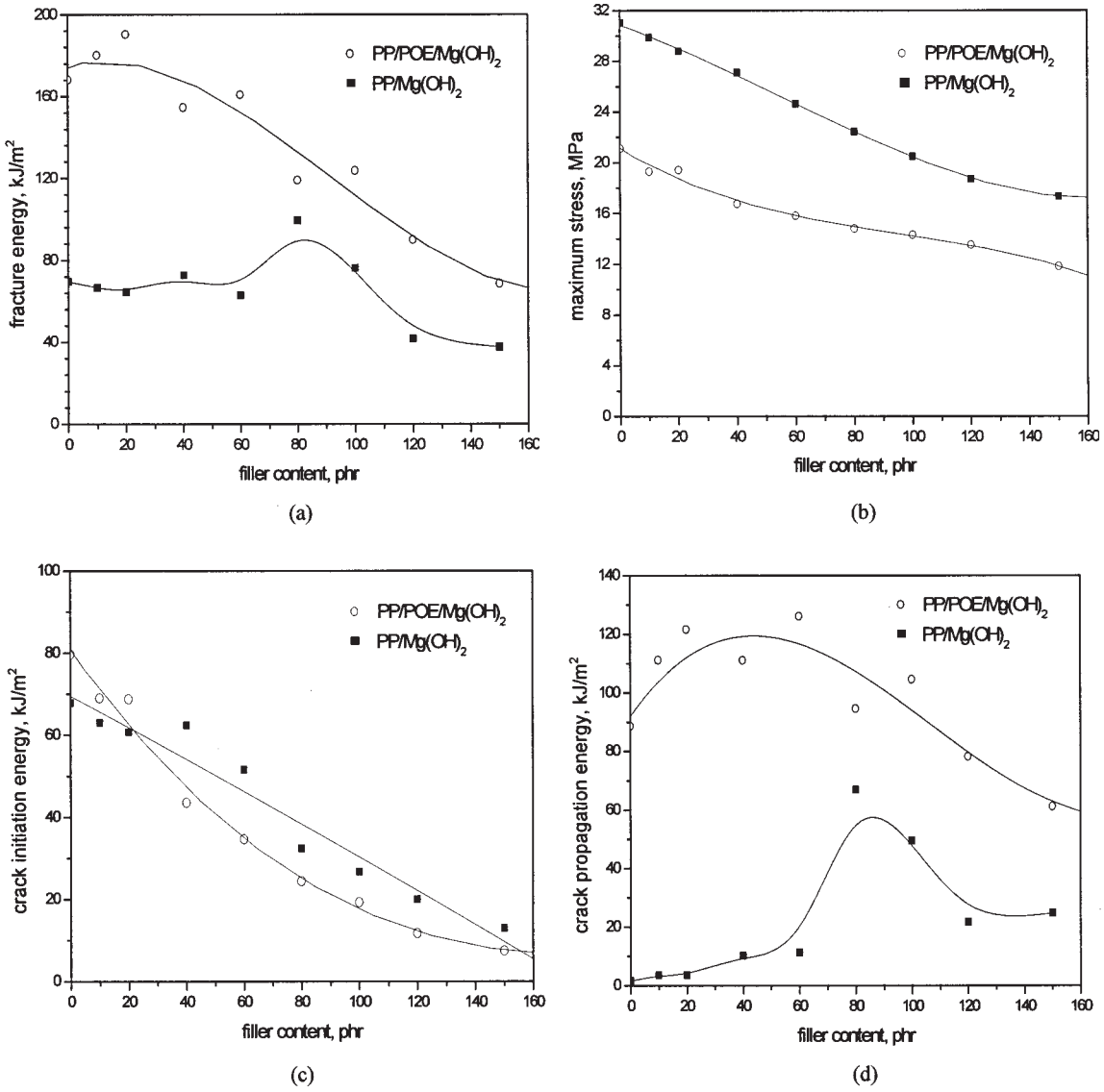

Figure 12 Energy and stress analysis based on the SENT test (1 mm/s) of PP composites and PP/POE (70/30) composites with various filler contents: (a) the total fracture energy versus the filler content, (b) the maximum stress versus the filler content, (c) the crack initiation energy versus the filler content, and (d) the crack propagation energy versus the filler content.

For the PP/POE composites with low POE contents, $Mg(OH)_2$ and POE particles dispersed separately in the matrix, and a few POE particles were observed in the region surrounding filler particles. Therefore, a separation microstructure existed in such composites. Even in the PP/POE (85/15 w/w) composites, POE-encapsulated filler particles could not be observed. This is contradictory with the observation of the impact-fracture surface, in which a fibrillation structure was confirmed [Fig. 7(c)]. With increasing POE content, the average size of POE increased, and the microstructures of the PP/POE composites remained in a separation manner. When the POE content reached a certain value, for example, 80/20 PP/POE, the average size of the POE particles remained constant. On the other hand, dark holes with irregular shapes were observed surrounding filler particles, as shown in Figure 13(e). The result indicates that the encapsulation microstructure formed in some PP/POE composites, and a separation microstructure existed simultaneously in the matrix. Therefore, a mixed microstructure of separation and encapsulation formed in the PP/POE composites with high POE contents. The distance between the POE particles continually decreased with further increasing POE content, and this was responsible for the brittle–ductile transition according to the percolation theory.

CONCLUSIONS

The toughness of the PP/POE/$Mg(OH)_2$ ternary composites strongly depended on the POE content. A

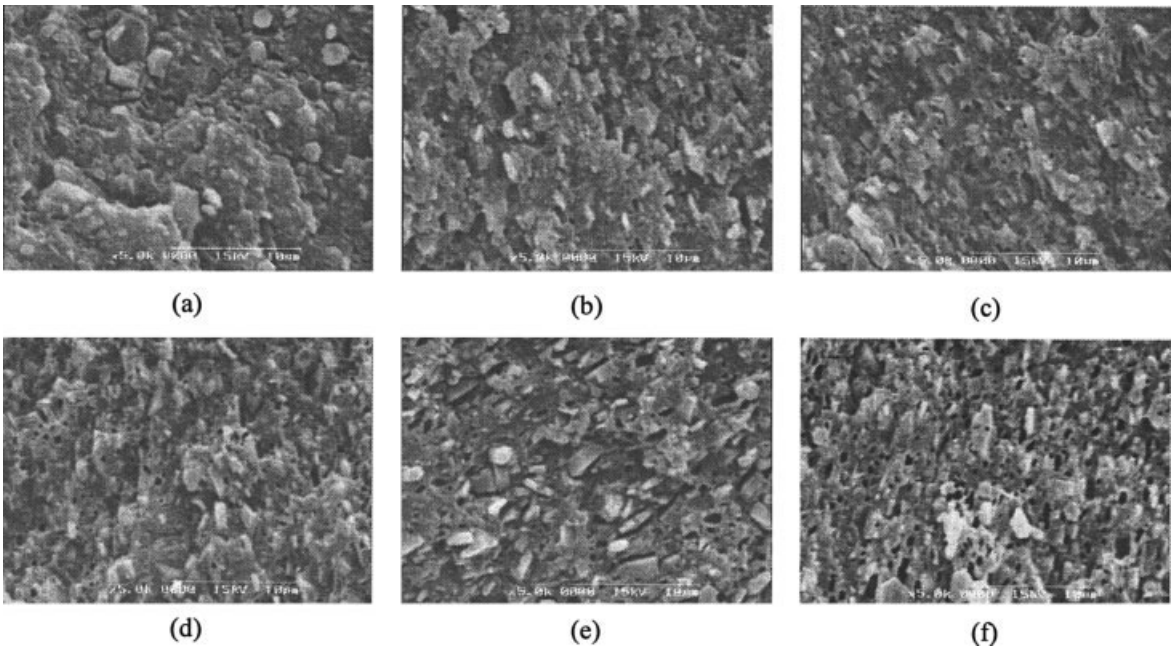

Figure 13 SEM micrographs of the etched surface of PP/POE/$Mg(OH)_2$ composites with various POE contents at a 5000× magnification: (a) PP/$Mg(OH)_2$ = 100/120, (b) PP/POE/$Mg(OH)_2$ = 90/10/120, (c) PP/POE/$Mg(OH)_2$ = 85/15/120, (d) PP/POE/$Mg(OH)_2$ = 80/20/120, (e) PP/POE/$Mg(OH)_2$ = 75/25/120, and (f) PP/POE/$Mg(OH)_2$ = 70/30/120.

brittle–ductile transition occurred in the PP/POE composites when POE reached a certain value. For PP/$Mg(OH)_2$ composites fractured in a brittle manner, stress whitening only occurred around the notch tip of impact-fractured specimens. The thickness of the stress-whitening zone increased with increasing POE content, and this indicated the improvement of POE in the plastic deformability of the polymer matrix. The $Mg(OH)_2$ content also influenced considerably the toughness of the PP/POE composites. The formation of microvoids caused by the debonding of $Mg(OH)_2$ particles could improve the plastic deformation of the polymer matrix ligaments. However, the improvement in the toughness of the PP/POE composites by $Mg(OH)_2$ was restricted by the poor interfacial adhesion between $Mg(OH)_2$ and the polymer matrix.

The influence of POE on the deformation mechanism of PP/POE composites might be considered from two aspects, that is, the $Mg(OH)_2$ particle debonding behavior and the deformability of the matrix. First, the existence of POE improved significantly the deformability of PP, resulting in extensive shear deformation of the polymer matrix during the deformation process. On the other hand, the interfacial adhesion between the polymer matrix and $Mg(OH)_2$ increased with the incorporation of POE. The formation of a fibrillation structure between the $Mg(OH)_2$ particles and polymer ligaments led to a change in the debonding mechanism of the $Mg(OH)_2$ particles.

TABLE I
POE Particle Size Analysis for the PP/POE/$Mg(OH)_2$ Composites

PP	POE	$Mg(OH)_2$	D_n (μm)	D_w (μm)	D_w/D_n
100	0	120	0	0	—
95	5	120	0.24	0.26	1.08
90	10	120	0.27	0.28	1.04
85	15	120	0.29	0.31	1.07
80	20	120	0.36	0.40	1.11
75	25	120	0.34	0.39	1.15
70	30	120	0.35	0.39	1.11

With the SENT test, it was possible to analyze the fracture behavior of the PP/POE/$Mg(OH)_2$ ternary composites. The incorporation of POE into the composites led to an increase in the fracture energy and a decrease in the maximum stress. The increase in the fracture energy was attributed to high energy dissipation during the crack propagation process due to the shear flow of the polymer matrix and fibrillation surrounding the filler particles. Because of the cavitation of POE at an early stage of the deformation process, the crack initiation energy of the PP/POE composites decreased with increasing POE content. The influence of the $Mg(OH)_2$ content on the fracture energy of the PP/POE composites was in agreement with the results of the notched impact test, which depended on the limited improvement in the polymer matrix deformability and the poor interfacial adhesion between the polymer matrix and $Mg(OH)_2$ particles.

A separation microstructure existed in the PP/POE composites with low POE contents. With increasing

POE content, the average size of POE increased, and the distance between the POE particles decreased. An encapsulation microstructure formed in the PP/POE composites with a certain POE content, and a separation microstructure existed simultaneously in the matrix.

References

1. Pukánszky, B.; Fekete, E. Adv Polym Sci 1999, 139, 109.
2. Pukanszky, B.; Tudos, F.; Kolarik, J.; Lednicky, F. Polym Compos 1990, 11, 98.
3. Long, Y.; Robert, A. J Appl Polym Sci 1996, 61, 1877.
4. Kolaþík, J.; Lednickù F. In Polymer Composites; Sedláèek, B., Ed.; de Gruyter: Berlin, 1986; p 537.
5. Chiang, W. Y.; Yang, W. D.; Pukánszky, B. Polym Eng Sci 1992, 32, 641.
6. Molnar, S.; Pukánszky, B.; Hammer, C. M.; Maurer, F. H. Polymer 2000, 41, 1529.
7. Pukanszky, B.; Tudos, F.; Kelen, T. Polym Compos 1986, 7, 106.
8. Kolarik, J.; Lednicky, F.; Jancar, J.; Pukanszky, B. Polym Commun 1990, 31, 201.
9. Jancar, J.; DiBenedetto, A. T. J Mater Sci 1994 29, 5651.
10. Wang, J.; Tung, J. F.; Ahmad Fuad, M. Y.; Hornsby, P. R. J Appl Polym Sci 1996, 60, 1425.
11. Dubnikova, I. L.; Berezina, S. M.; Antonov, A. V. J Appl Polym Sci 2002, 85, 1911.
12. van del Wal, A.; Gaymans, R. J. Polymer 1999, 40, 6057.
13. Dijkstra, K.; Laak, J.; Gaymans, R. J. Polymer 1994, 35, 315.
14. Wu, S. Polymer 1985, 26, 1855.
15. Wu, S. J Appl Polym Sci 1988, 35, 549.
16. Muratoglu, O. K.; Argon, A. S.; Cohen, R. E. Polymer 1995, 36, 2143.
17. Kim, G. M.; Micher, G. H. Polymer 1998, 39, 5699.
18. Pukanszky, B.; Belina, K.; Rockenbauer, A.; Maurer, F. H. J. Composites 1994, 25, 205.
19. Pukanszky, B.; Fekete, E.; Tüdos, F. Makromol Chem Macromol Symp 1989, 28, 165.
20. Pukanszky, B.; Voros, G. Compos Interfaces 1993, 1, 411.
21. Dijkstra, K.; Bolscher, G. H. J Mater Sci 1994, 29, 3489.